Feasibility Study of Real-Time Carbon Emission Responsive Electric Vehicle Charging Control in Buildings

Preprint

Jing Wang, Rawad El Kontar, Xin Jin, and Jennifer King

National Renewable Energy Laboratory

Presented at the 2022 ACEEE Summer Study on Energy Efficiency in Buildings
Pacific Grove, California
August 21-26, 2022

NREL is a national laboratory of the U.S. Department of Energy
Office of Energy Efficiency & Renewable Energy
Operated by the Alliance for Sustainable Energy, LLC

This report is available at no cost from the National Renewable Energy Laboratory (NREL) at www.nrel.gov/publications.

Contract No. DE-AC36-08GO28308

Conference Paper
NREL/CP-5500-82437
September 2022

Feasibility Study of Real-Time Carbon Emission Responsive Electric Vehicle Charging Control in Buildings

Preprint

Jing Wang, Rawad El Kontar, Xin Jin, and Jennifer King

National Renewable Energy Laboratory

Suggested Citation
Wang, Jing, Rawad El Kontar, Xin Jin, and Jennifer King. 2022. *Feasibility Study of Real-Time Carbon Emission Responsive Electric Vehicle Charging Control in Buildings: Preprint*. Golden, CO: National Renewable Energy Laboratory. NREL/CP-5500-82437. https://www.nrel.gov/docs/fy22osti/82437.pdf.

NREL is a national laboratory of the U.S. Department of Energy
Office of Energy Efficiency & Renewable Energy
Operated by the Alliance for Sustainable Energy, LLC

This report is available at no cost from the National Renewable Energy Laboratory (NREL) at www.nrel.gov/publications.

Contract No. DE-AC36-08GO28308

Conference Paper
NREL/CP-5500-82437
September 2022

National Renewable Energy Laboratory
15013 Denver West Parkway
Golden, CO 80401
303-275-3000 • www.nrel.gov

NOTICE

This work was authored by the National Renewable Energy Laboratory, operated by Alliance for Sustainable Energy, LLC, for the U.S. Department of Energy (DOE) under Contract No. DE-AC36-08GO28308. Funding provided by NREL's Laboratory Directed Research and Development program. The views expressed herein do not necessarily represent the views of the DOE or the U.S. Government. The U.S. Government retains and the publisher, by accepting the article for publication, acknowledges that the U.S. Government retains a nonexclusive, paid-up, irrevocable, worldwide license to publish or reproduce the published form of this work, or allow others to do so, for U.S. Government purposes.

This report is available at no cost from the National Renewable Energy Laboratory (NREL) at www.nrel.gov/publications.

U.S. Department of Energy (DOE) reports produced after 1991 and a growing number of pre-1991 documents are available free via www.OSTI.gov.

Cover Photos by Dennis Schroeder: (clockwise, left to right) NREL 51934, NREL 45897, NREL 42160, NREL 45891, NREL 48097, NREL 46526.

NREL prints on paper that contains recycled content.

Feasibility Study of Real-Time Carbon Emission Responsive Electric Vehicle Charging Control in Buildings

Jing Wang, Rawad El Kontar, Xin Jin, Jenifer King
National Renewable Energy Laboratory

ABSTRACT

With the progressing electrification of the transportation sector, the source of carbon emissions is gradually shifting from fossil fuel to grid electricity because of electric vehicles (EVs). The carbon intensity of the grid can fluctuate significantly within hours due to the time-varying power generation mix. Therefore, shifting EV charging loads to cleaner hours in response to the carbon intensity signals can reduce carbon emissions. Existing EV charging control methods typically consider the electricity price or the available generation by distributed energy resources (e.g., photovoltaics) to inform decision-making. Such methods tend to reduce energy costs but may neglect the environmental impact of EV charging activities. We propose and compare four carbon emission responsive EV charging controllers with various control rules. The proposed controllers are evaluated based on simulation experiments using metrics such as carbon emission reduction potential, state of charge (SOC) at departure, and peak demand. We found that the need of EV owners to have full batteries at departure could lead to an emission increase when the curtailed EV charge was compensated before departure. Further, up to 12.7% of carbon emission reduction can be achieved if the EV owners reduce the target SOC at departure by less than 15%.

Introduction

In the United States, the transportation sector accounted for 36% of the total energy-related carbon dioxide (CO_2) emissions in 2020 (U.S. Energy Information Administration, 2022). Given the continued increase in electric vehicle (EV) penetration, the transportation sector will develop a higher dependence on the electric power sector for EV charging. Moreover, the time-varying generation mix of the power grid leads to significant fluctuations in the carbon emission intensity within hours. Therefore, shifting EV charging loads to cleaner hours in response to carbon intensity signals can reduce carbon emissions and help achieve the United States' decarbonization goal.

To date, most EV charging control algorithms have been designed either to reduce charging costs or to better utilize renewable energy generation. Liu et al. (2019) proposed a transactive real-time EV charging management scheme for commercial buildings with on-site PV generation. The controller scheduled its net electricity exchange with the grid under uncertainties of PV generation and EV parking to maximize its profit. Huang et al. (2019) reported a case study of a residential cluster with photovoltaics (PV), centralized heat pumps, thermal energy storage, and EVs. The genetic algorithm was adopted for maximizing the self-consumption rate of the locally generated energy. Babaei et al. (2020) proposed a demand-side management approach based on the predetermined hourly generation and time-varying tariffs to enhance the reliability and quality of standalone energy systems. Mixed-integer linear programming was adopted to optimally manage the renewable generation, battery, and EV.

More recently, an increasing interest has been identified in integrating grid carbon intensity data into EV charging control studies. Shi and Karimzadeh (2021) conducted the analysis using location- and time-based grid power mix data with in-field EV charging data to discover the carbon emissions of common EV charging patterns. They concluded that optimizing EV charging for carbon intensity would yield 8-14% reductions in related carbon emissions across 44 states in the United States. Dixon et al. (2020) applied optimal EV charging scheduling to minimize carbon emissions while maximizing the absorption of excess wind energy generation. Between $35gCO_2$/km to $56gCO_2$/km EV emissions were achieved through the proposed charging scheduling algorithm.

Besides the optimization-based controls discussed above, many works focus on the development of rule-based EV charging control, considering their simplicity and broadness in deployment with comparable performance to optimal control when designed carefully. Khemakhem et al. (2020) developed a supervisory control logic for smoothing residential home power profiles through EV charging and discharging control. The coordination among the EVs, the home load profile, and the load profiles of the neighbors was taken into consideration. Shanti et al. (2020) discussed the modeling and control of integrated EV charging infrastructure in buildings and mixed-use communities. An EV charging control logic according to the solar irradiance and its trend is adopted to better align the EV charging loads with the PV generation. Zhou and Cao (2019) compared various dynamic grid-responsive control strategies for PV and EV. Different off-peak electricity tariffs and rated renewable capacities were compared in terms of their ability to provide energy flexibility.

To the best of the authors' knowledge, no rule-based control study has been performed to explore the feasibility of EV charging in response to the time-varying carbon intensity of the grid. This paper compares the performance of several carbon responsive EV charging controllers regarding their decarbonization potential and peak demand. A simulation experiment has been conducted on a mixed-use community in Denver, Colorado. Through the comparison, the impact of control thresholds, range anxiety, and maximum charging power limit is discussed. According to the authors' earlier studies on carbon-responsive building control (Wang, et al., 2022), rule-based controllers can reduce a home's annual carbon emissions by 6.0% to 20.5%. Therefore, this work applies rule-based controllers to EV charging as a preliminary effort to facilitate the investigation of decarbonization control design for EVs. The main contributions of this work are:

- Development of EV charging controllers in response to the real-time grid carbon emission intensity signal;
- Simulation-based evaluation of the proposed controllers on different building EV loads;
- Qualitative and quantitative discussion of the trade-offs between carbon emission, state of charge (SOC) at departure, and peak demand.

The remainder of this paper is organized as follows: The Methodology section presents the research methodology of the proposed rule-based carbon responsive control framework. The Case Study section describes the building and EV load models, as well as the simulation inputs for the case study. The Results and Discussions section discusses the simulation results with the metrics of annual carbon emission and peak power. The Conclusion section concludes the work and recommends future topics for further study.

Methodology

The concept of carbon emission responsive EV charging control is to enable load shifting from hours of high grid carbon intensity to those of low carbon intensity so that the total carbon

emissions during a given period are reduced. To determine whether an hour has "clean" energy (i.e., low carbon intensity) or "unclean" (i.e., high carbon intensity), this paper adopts a three-range categorization method. Two carbon intensity thresholds—higher threshold (HT) and lower threshold (LT)—are adopted. If an hour has a carbon intensity value (unit: kg $CO_{2e.q.}$/MWh) that is higher than the HT, it is then classified as the unclean hour, and vice versa. The vehicle owners' range anxiety, which is the need to have a full battery at departure, is accounted for through the compensation for EV load curtailment in the last two hours before departure. In this work, we assume that the EV arrival and departure times align with the corresponding building operation hours that they are attached to. We only implemented the control every day during those operation hours. EV loads outside those control hours still exist but are comparatively less and are thus uncontrolled.

Figure 1 shows the flow chart of the proposed charging controller, which repeats daily. At the first timestep of the day, the controller determines if the current timestep belongs to the controlled hours ranging from t_{start} to t_{end}. If it doesn't, the originally scheduled EV power $P^t_{schedule}$ based on the prediction will be adopted for the current timestep. If the current timestep belongs to the controlled hours, the controller proceeds to the EV control. Note that at the beginning timestep of the control t_{start}, the total curtailed EV energy $E^t_{curtailed}$ is reinitialized as zero for the current control cycle. When the timestep proceeds into the carbon emission responsive control hours, the current grid electricity carbon intensity value is compared with the predetermined HT and LT to determine the control action. For the unclean hour, a zero EV charging power is dictated. For the hour that lies in between the HT and LT, an EV power P^t is calculated with the following equation:

$$P^t = r * P^t_{schedule}, \tag{1}$$

where the $P^t_{schedule}$ is the originally scheduled EV power based on the prediction; r is the charge ratio obtained by:

$$r = 1 - \frac{e^t - LT}{HT - LT}. \tag{2}$$

In Equation (2), e^t represents the grid emission intensity at the current timestep t. Note that r has a range of 0~1, meaning that the effective EV power will be less than or equal to the originally scheduled EV load. This ensures that when the carbon intensity is larger than LT, EV load will be curtailed. The closer it is to HT (i.e., unclean), the smaller the EV power.

For the clean hours, a load compensation for the accumulated curtailed EV energy for the day will be implemented. The power for curtailment compensation is calculated by:

$$P^t = P^t_{schedule} + \frac{E^t_{curtailed}}{\Delta t}, \tag{3}$$

where $E^t_{curtailed}$ is the accumulated curtailed EV energy for the day until the current timestep, Δt is the control timestep. During the compensation, the effective EV power P^t is larger than the scheduled power $P^t_{schedule}$. In this way, the EV load is shifted from the unclean hours to the clean hours.

Another type of load compensation happens during the last two hours before the EV departure time. Similar to Equation (3), the compensation power is calculated by:

$$P^t = P^t_{schedule} + \frac{E^t_{curtailed}}{t_{end} - t}, \tag{4}$$

where t_{end} is the EV departure time (assumed to be the same as building operation end hour) and t is the current time. From Equations (3) and (4), it can be inferred that the lower limit of P^t is $P^t_{schedule}$. However, to mitigate the potential peak demand increase issue due to EV load shifting, an upper limit for P^t is set in some controllers for comparison. The effective EV charging power cannot exceed the maximum charging power of the EV charger, which varies with the building size.

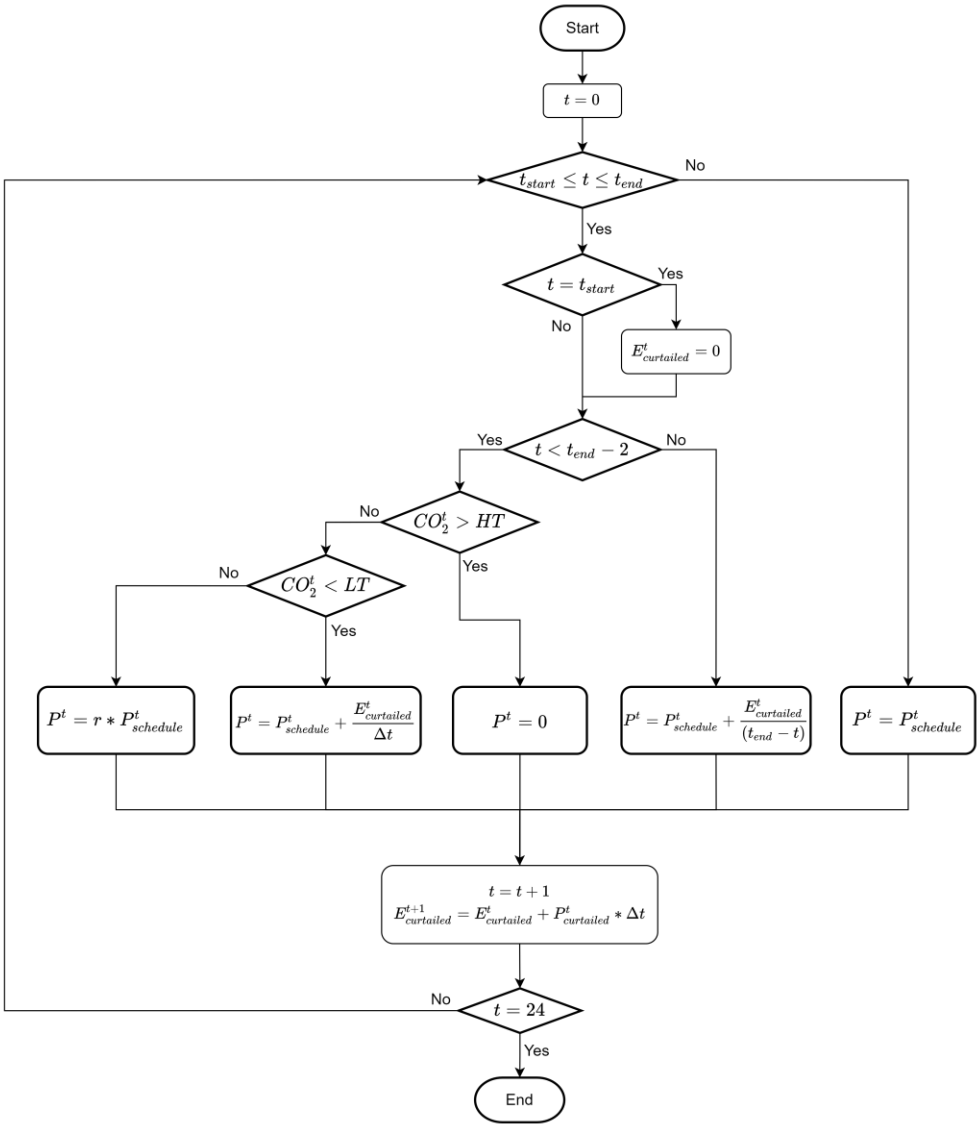

Figure 1. Flow chart of the proposed carbon emission responsive EV charging controller.

Table 1 lists the different configurations of the carbon emission responsive controllers studied in this work. Controller 1 sets the baseline of all controllers, where the lower threshold value is 40% of the annual carbon intensity range and the higher threshold is 60%. Compensation for curtailed EV energy before departure time is involved in the base control. No charging power upper limit is implemented in this control. In Controller 2, we modified the thresholds to 30% and 70% to investigate the impact of control rules. In Controller 3, we removed the load compensation

before EV departure based on Controller 2. This allows the impact analysis of the last-minute compensation. Finally, in Controller 4, we added an upper limit for EV charging power on top of Controller 3 to discuss its effect on EV peak demand. Such sequential variation design of the controller configurations allows us to analyze one impact factor of EV charging control at a time.

Table 1. Configurations of proposed EV charging controllers.

Controller Configuration	Thresholds	Compensation Before Departure	Charging Power Limit
1 (Base control)	40%/60%	Yes	No
2 (Adjusted rules)	30%/70%	Yes	No
3 (No compensation)	30%/70%	No	No
4 (Power limit)	30%/70%	No	Yes

Case Study

The proposed carbon emission responsive controllers were tested on the EV charging loads of a mixed-use community (Figure 2) in Denver, Colorado. The community is currently under construction and will have 148 buildings, most of which are large commercial buildings including offices, shopping malls, retail stores, hotels, schools, hospitals, etc. All residential buildings in this community are multifamily buildings.

Figure 2. Three-dimensional rendering map of the mixed-use community (Wang, et al., 2022).

We used URBANopt™ (El Kontar, et al., 2020) to build a high-fidelity physics-based model for all buildings in this community. The EV charging load is modeled as static load profiles, which were created for a Denver district to reflect different EV charging behavior (Pless, et al., 2020). The building types in the case study community were mapped into three charging station types: residential, public, and workplace. The different charging behaviors (e.g., business as usual, free workplace charging) were stochastically assigned to each building. More information about URBANopt's EV modeling capability can be found in the reference (National Renewable Energy Laboratory, 2021). The EV charging controller proposed in this work is implemented through an OpenStudio™ Energy Management System measure. We note that since the detailed charging events and EV batteries are not modeled, the SOC at departure in this work is defined as the percentage of the total charged EV energy over the originally scheduled EV charging energy.

The grid carbon emission intensity data were adopted from the Cambium 2021 data set (Gagnon, et al., 2021). Specifically, the short-run marginal $CO_{2e.q.}$ emission rate data for the year 2022 was used. Marginal carbon emissions represent the emissions that would come online if any new load was added (Listgarten, 2019) and it is thus often used in informing control decisions. While the short-run marginal rate only accounts for the operational changes posed to the grid, the long-run marginal rate also considers the structural change of the grid such as the expanded renewable energy integration. Figure 3 compares the short-run and long-run marginal signals for 2022. We see that the short-run data present a higher carbon intensity and more daily and seasonal fluctuations than the long-run data. In this paper, we chose the short-run data as our control input while noting that the choice of short-run versus long-run signals is under debate and is out of this paper's scope.

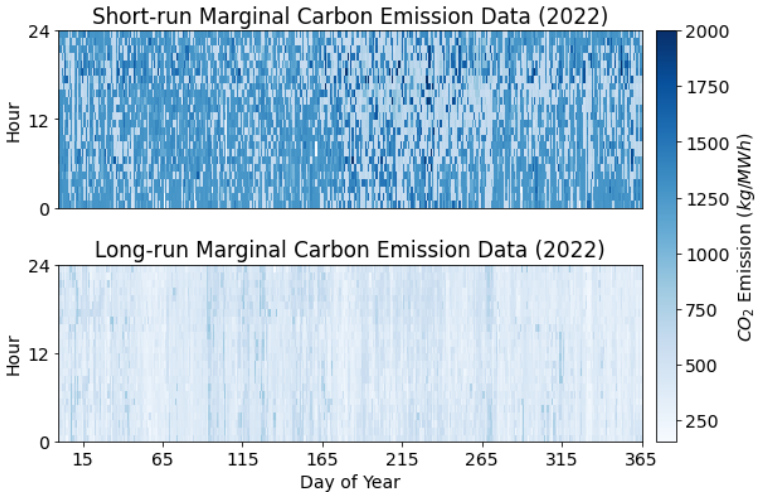

Figure 3. Short-run versus long-run marginal carbon emission data from Cambium.

Annual simulation with an hourly timestep was run for the case study community in 2022. Typical Meteorological Year 3 weather data for Denver was used. Given the page limit of this paper, the simulation results for 10 different buildings, one from each building type in the community, will be discussed as a proof of concept. More aggregated results for the whole community will be included in a future journal publication.

Results and Discussions

This section presents the results from the simulation experiments and discusses the results with regard to the charging behavior, annual carbon emissions, and peak demand.

Charging Behavior

Figure 4 shows the EV charging behaviors of the strip shopping mall building on a summer weekday as an example. The four plots represent the four controllers. The first subplot at the top shows the grid carbon emission intensity, which is the same across all controllers. The middle subplot shows the charge state of the EV, where the value of 0~1 means EV load is curtailed based on the charge ratio obtained from Equation (2). The charge state 2 means compensation for EV curtailment, and 3 means charging at the originally scheduled EV power. The bottom subplot shows the original EV power without control versus the effective power with various controllers.

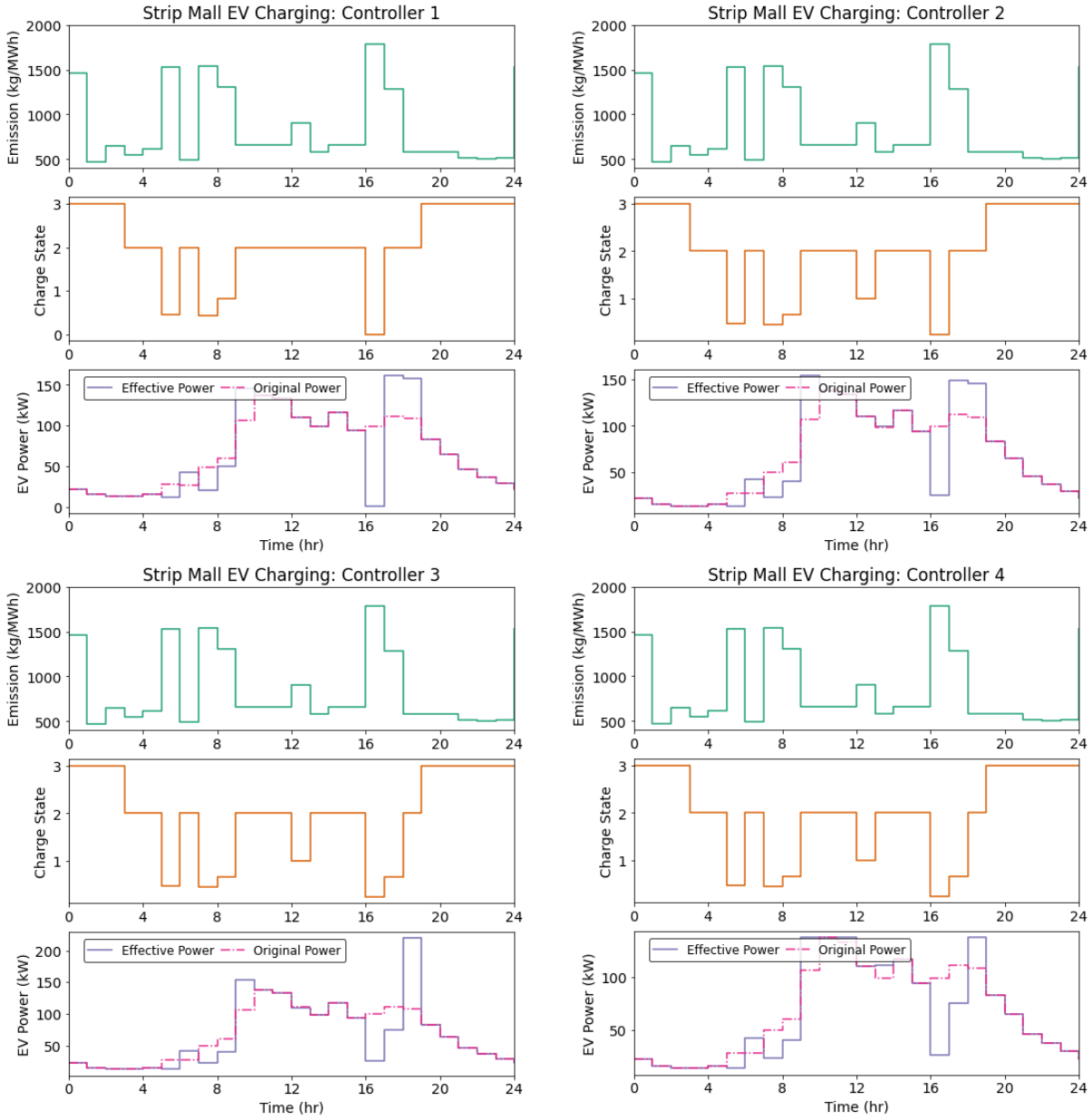

Figure 4. Comparison of EV charging behavior in strip shopping malls across different controllers.

Comparing Controllers 1 and 2 that have different control thresholds, we see that the same carbon intensity value tends to be classified as clean easier in Controller 1, which has a higher LT value (1,196.68 kg/MWh) than Controller 2 (897.51 kg/MWh). For instance, at 12 PM, the carbon intensity of 901.9 kg/MWh is considered clean in Controller 1 while unclean in Controller 2. This leads to a slight EV curtailment in Controller 2. Figure 5 plots the relationship between charge ratio r and the carbon intensities under different control rule settings. At the carbon intensity of around 1,500 kg/MWh, the two rules have the same charge ratio. Below 1,500, Controller 1 has a larger charge ratio, which corresponds to less curtailment (i.e., load shifting), and vice versa. Therefore, the actual carbon emissions reduction potential of the two controllers is dependent on

the frequency distribution of the annual carbon intensities of the grid. More discussion on this is in the following subsection.

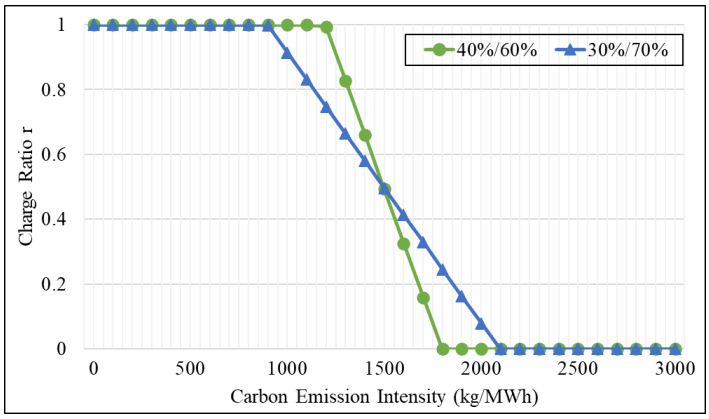

Figure 5. Values of charge ratio r at varying carbon emission intensities under different control rules.

Controllers 2 and 3 have the same control thresholds, but no last-minute compensation was implemented in Controller 3. From Figure 4, we notice that during hours 17 and 18, Controller 2 has a relatively even EV power as the total curtailed EV energy was compensated evenly during the last two hours before departure. However, in Controller 3, the EV load was first curtailed at hour 17 due to the high carbon emission intensity and then compensated at hour 18, where the intensity drops below the LT. The different charging behavior has led to a different carbon emissions reduction potential, as well as a different battery SOC at departure. Additionally, Controller 3 has a higher peak power than Controller 2 as the compensation for curtailment happened in a shorter period of one hour rather than two hours. This peak demand increase is mitigated in Controller 4, where an upper EV charging power limit is introduced.

Annual Carbon Emissions

Figure 6 plots the annual carbon emission changes of different charging controllers compared to no controller. From the figure, we see similar trends of carbon emissions across different building types. In Controllers 1 and 2, the annual carbon emissions increased compared to when there is no EV charging control. This has been caused by the mechanism of last-minute compensation, in which much of the earlier curtailed EV energy was shifted to the last two hours before EV departure. However, those two hours are not necessarily with the lowest carbon intensities. As a result, compensating during the last two hours turned out to cancel out the carbon emission reductions from EV load shifting from unclean to clean hours. More specifically, Controller 1 with the 40%/60% thresholds has an even higher carbon emission increase than Controller 2 with the 30%/70% rule. This is because, during the whole year, most carbon emission intensities fall into the range below 1,500 kg/MWh (see Figure 7). This has led to a higher average charge ratio with Controller 1 (see Figure 5). Therefore, less EV load is shifted from high carbon intensity hours to low carbon intensity hours under Controller 1. Hence, a higher carbon emissions increase is seen.

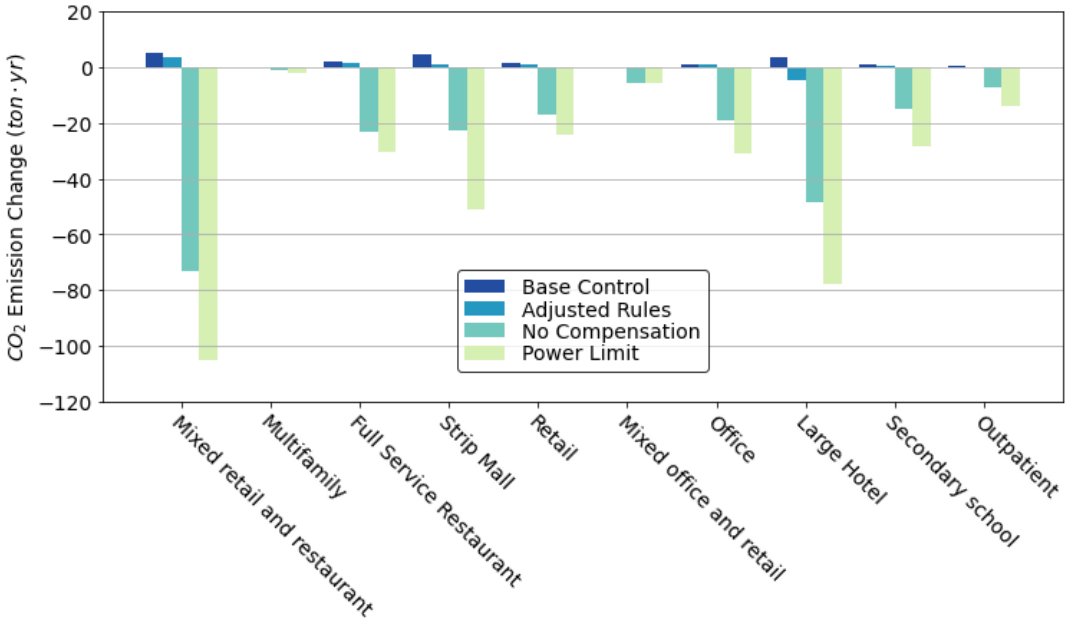

Figure 6. Annual carbon emission changes of different charging controllers compared to no controller (negative value means carbon reduction).

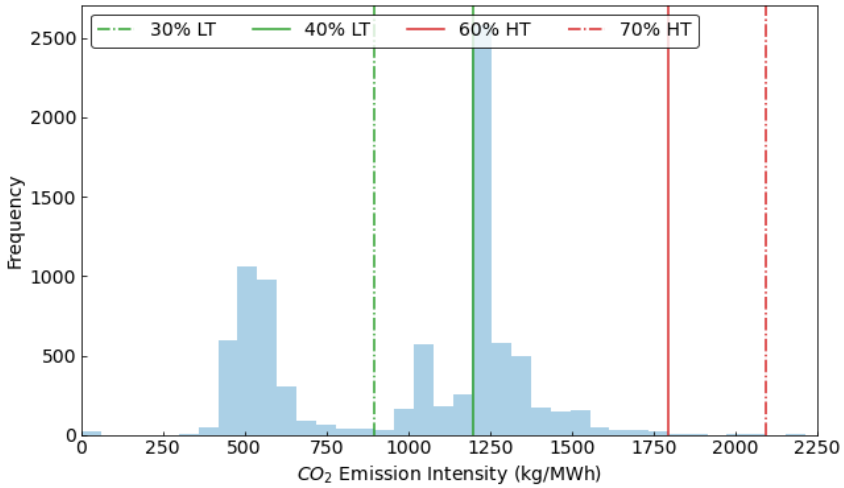

Figure 7. Histogram of carbon emission intensities over the year 2022.

In scenarios with Controller 3, large carbon emission reductions are seen compared to no controller. The emission reductions range from 3.2% in the mixed office and retail building to 7.0% in the office building. This can be attributed to the fact that Controller 3 did not include last-minute compensation. Hence, EV curtailment compensation only happens when the grid carbon intensity is low. This ensures that EV load is shifted from the high carbon hours to low carbon hours. Though the battery SOC at departure is not guaranteed to be at 100%, the loss of battery SOC is traded off for emission reductions.

Finally, in Controller 4 where we added an upper power limit for EV charging, we see more carbon reductions—ranging from 3.4% in the mixed office and retail building to 12.7% in the secondary school. This is because the limit on maximum charging power further constrained

the energy charged into the battery during the curtailment compensation. As a result, the battery SOC at EV departure will further decrease while the carbon emission reductions rise.

Table 2 lists the annual average EV battery SOC at departure for the four charging controllers. In Controllers 1 and 2, full battery at departure is guaranteed, where the SOC equals 1. In Controllers 3 and 4, we see a trade-off of battery SOC for carbon emission reductions. Controller 4 has a lower SOC than Controller 3 given the maximum charging power limit. Overall, the SOC at departure is maintained above 85% for all buildings. Note that the large hotel building is marked as N/A because it is operated 24 hours a day, so no EV departure hour can be identified for SOC evaluation.

Table 2. Annual average EV battery SOC at departure of different charging controllers.

Building	Controller 1	Controller 2	Controller 3	Controller 4
Mixed retail and restaurant	1	1	0.93	0.91
Multifamily	1	1	0.95	0.93
Full service restaurant	1	1	0.93	0.92
Strip mall	1	1	0.96	0.92
Retail	1	1	0.93	0.91
Mixed office and retail	1	1	0.94	0.85
Office	1	1	0.93	0.90
Large hotel	N/A	N/A	N/A	N/A
Secondary school	1	1	0.93	0.89
Outpatient	1	1	0.93	0.89

Peak Demand

Figure 8 plots the monthly EV peak demand of the four controllers. In the plots, the colored boxes represent the distribution of the monthly peak demands with controllers, and the black bars represent the peak demands without control. Because the original EV loads were modeled as static load profiles and no seasonal changes were included in the modeling, the original monthly peak demand only has one single value for each building.

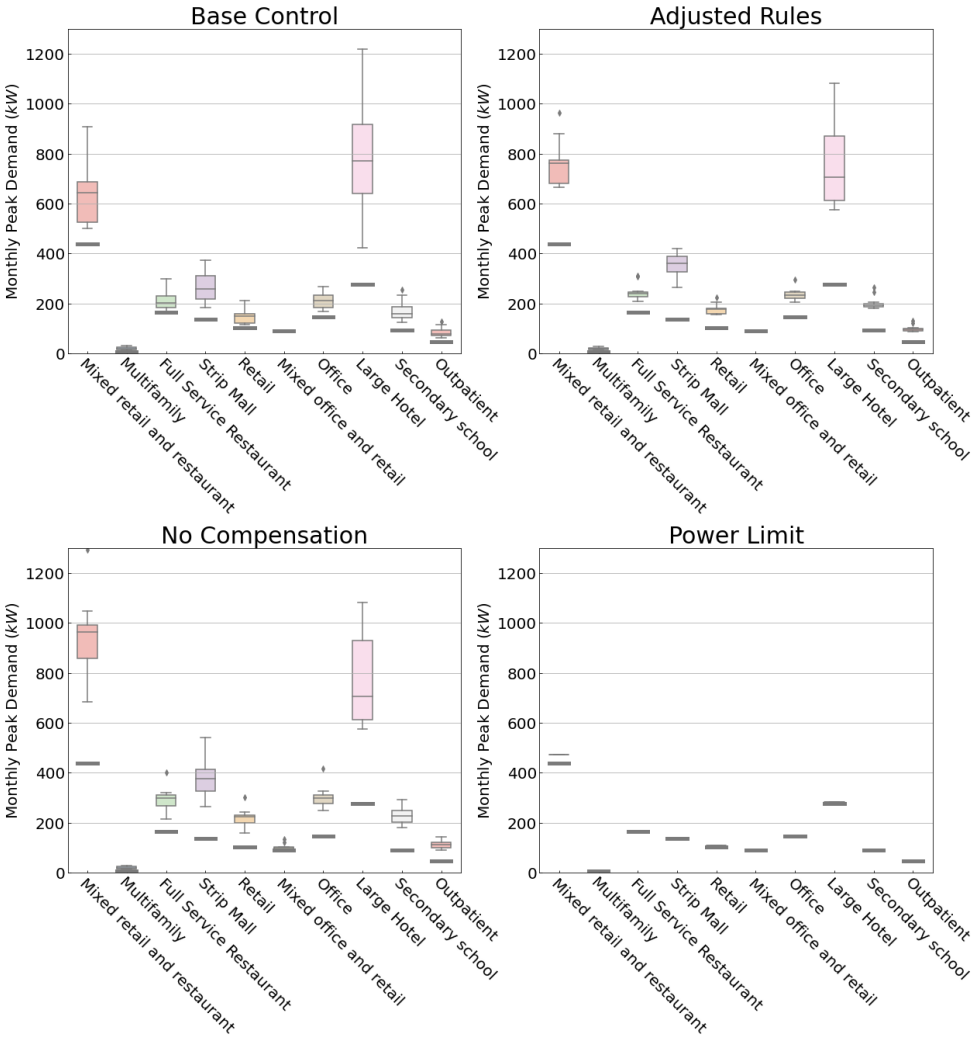

Figure 8. Monthly peak EV demand boxplots for different controllers.

Based on the figure, we see an overall trend of peak demand increasing from Controller 1 to Controller 3. This can be attributed to the fact that Controller 1 has a higher average charge ratio than Controller 2, which makes the shifted EV loads smaller. The smaller shifted loads lead to smaller peak demand. In Controller 3, where the last-minute load compensation was taken out, the peak demand further increases because of the controller design shown in Figure 1. When no last-minute load compensation is available, most of the curtailed EV energy is compensated whenever the grid carbon intensity is considered clean and the compensation takes place in one timestep. This has led to relatively higher peak demands than the last-minute compensation, which happens evenly in two timesteps. This limitation of the control algorithm can be mitigated if the forecast of the grid carbon intensity is available. In Controller 4, the peak demands with and without charging control overlap with each other because an upper limit of the charging power was set to be at the EV charger capacity value.

It is also noticed that the large hotel building shows a different trend of peak demand among controllers. Controller 1 in the large hotel had several high peaks above 1,200 kW. This has been caused by consecutive unclean hours followed by a clean hour, where the large curtailed EV energy has been compensated at once. This was not witnessed in Controller 2 in the large hotel due to

their different threshold settings, where a clean hour in Controller 1 is not necessarily considered clean in Controller 2. Controllers 2 and 3 in the large hotel generally have the same peak demand values in most months except for February, where an EV load compensation power was doubled in Controller 3 during the last two hours due to the removal of last-minute compensation.

To further investigate the trade-offs between carbon emission reduction, SOC at departure, and peak demand, a bubble plot is shown in Figure 9. The x-axis represents carbon emission reductions based on results without charging control. The y-axis represents the EV battery SOC at departure. The diameters of the bubbles showcase the values of the peak demand. From the figure, the correlation between carbon emission reductions and SOC at departure can be approximately described as a linear relationship. The higher the emission reductions, the lower the SOC at departure. Their correlation to the peak demand is less explicit. Controller 4 with the highest carbon emission reductions tends to have the lowest peak demand but for Controller 3, the correlation is reversed. This depends on how the controller constraints are designed.

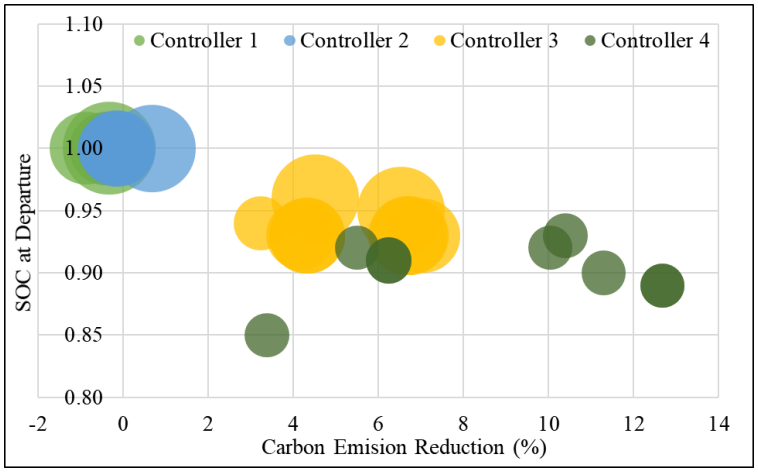

Figure 9. Correlations between carbon emission reduction, SOC at departure, and peak demand (as indicated by the diameter of the bubbles).

Conclusion

In this work, we proposed and compared four carbon emission responsive EV charging controllers with various control rules. The proposed controllers were evaluated based on simulation experiments in terms of their carbon emission reduction potential, SOC at departure, and peak demand. Through the qualitative and quantitative evaluation, we found that the need of EV owners to have full batteries at departure could lead to an emission increase when the curtailed EV charge was compensated before departure. Further, lowering the target battery SOC at departure by less than 15% can lead to up to 12.7% of carbon emission reduction depending on the building type. EV charging control caused higher EV peak demand, but this can be mitigated by constraining the upper charging power limit of the charging events. In the future, we plan to further improve the controllers by introducing forecasts of carbon emission intensities to enable predictive control. More constraints such as the lower limit for battery SOC can be investigated to further improve the control performance and alleviate range anxiety.

Acknowledgment

This work was authored by the National Renewable Energy Laboratory, operated by Alliance for Sustainable Energy, LLC, for the U.S. Department of Energy (DOE) under Contract No. DE-AC36-08GO28308. Funding provided by NREL's Laboratory Directed Research and Development program. The views expressed in the article do not necessarily represent the views of the DOE or the U.S. Government. The U.S. Government retains and the publisher, by accepting the article for publication, acknowledges that the U.S. Government retains a nonexclusive, paid-up, irrevocable, worldwide license to publish or reproduce the published form of this work, or allow others to do so, for U.S. Government purposes. The authors would like to gratefully acknowledge Kalpesh Chaudhari, Joshua Comden, Dylan Wald, Brian Ball, and Amy Allen for their insights and discussions during the development of this work.

References

Babaei, M., Azizi, E., Beheshti, M. T. & Hadianb, M., 2020. Data-Driven load management of stand-alone residential buildings including renewable resources, energy storage system, and electric vehicle. *Journal of Energy Storage,* Volume 28, p. 101221.

Dixon, J., Bukhsh, W., Edmunds, C. & Bell, K., 2020. Scheduling electric vehicle charging to minimise carbon emissions and wind curtailment. *Renewable Energy*, Volume 161, pp. 1072-1091.

El Kontar, R. et al., 2020. *URBANopt: An Open-Source Software Development Kit for Community and Urban District Energy Modeling*, Golden, CO: National Renewable Energy Laboratory (NREL).

Gagnon, P. et al., 2021. *Cambium data for 2021 Standard Scenarios.* [Online]
Available at: https://cambium.nrel.gov/
[Accessed 11 March 2022].

Huang, P. et al., 2019. Transforming a residential building cluster into electricity prosumers in Sweden: Optimal design of a coupled PV-heat pump-thermal storage-electric vehicle system. *Applied Energy*, Volume 255, p. 113864.

Khemakhem, S., Rekik, M. & Krichen, L., 2020. A collaborative energy management among plug-in electric vehicle, smart homes and neighbors' interaction for residential power load profile smoothing. *Journal of Building Engineering,* Volume 27, p. 100976.

Listgarten, S., 2019. *When to use Marginal Emissions (and when not to).* [Online]
Available at: https://www.paloaltoonline.com/blogs/p/2019/09/29/marginal-emissions-what-they-are-and-when-to-use-them
[Accessed 11 March 2022].

Liu, Z. et al., 2019. Transactive Real-Time Electric Vehicle Charging Management for Commercial Buildings With PV On-Site Generation. *IEEE Transactions on Smart Grid*, 10(5), pp. 4939-4950.

National Renewable Energy Laboratory, 2021. *URBANopt Documentation - EV Charging Scenario.* [Online]
Available at: https://docs.urbanopt.net/resources/scenarios/evcharging.html#ref1
[Accessed 11 March 2022].

Pless, S. et al., 2020. *Integrating Electric Vehicle Charging Infrastructure into Commercial Buildings and Mixed-Use Communities: Design, Modeling, and Control Optimization Opportunities*, Golden, CO: National Renewable Energy Laboratory (NREL).

Shi, W. & Karimzadeh, M., 2021. *Automating load shaping for EVs: optimizing for cost, grid constraints, and… carbon?,* s.l.: Sense Labs, Inc.

U.S. Energy Information Administration, 2022. *In 2020, the United States produced the least CO2 emissions from energy in nearly 40 years.* [Online]
Available at: https://www.eia.gov/todayinenergy/detail.php?id=48856

Wang, J., El Kontar, R., Jin, X. & King, J., 2022. Electrifying High-Efficiency Future Communities: Impact on Energy, Emissions, and Grid. *Advances in Applied Energy.*

Wang, J. et al., 2022. Carbon Emission Responsive Building Control: A Case Study With an All-Electric Residential Community in a Cold Climate. *Applied Energy.*

Zhou, Y. & Cao, S., 2019. Energy flexibility investigation of advanced grid-responsive energy control strategies with the static battery and electric vehicles: A case study of a high-rise office building in Hong Kong. *Energy Conversion and Management,* Volume 199, p. 111888.